

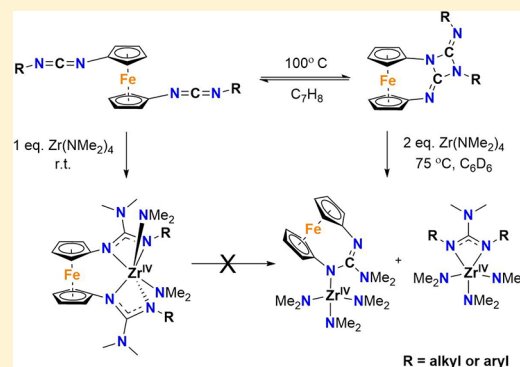
1,1'-Dicarbodiimidoferrocenes: Synthesis, Characterization, and Group IV 1,1'-Bisguanidinateferrocene Complexes

Orhi Esarte Palomero and Richard A. Jones*[✉]

Department of Chemistry, The University of Texas at Austin, Austin, Texas 78712-1224, United States

S Supporting Information

ABSTRACT: We report the two-step one-pot preparation of a series of bulky substituted 1,1'-dicarbodiimidoferrocene *proligands*. In solution the compounds achieve equilibrium with the corresponding 2,4-diimino-1,3-azetidines products which exhibit distinct spectroscopic and electrochemical features. Metalation of the carbodiimides with $M(\text{NMe}_2)_4$ ($M = \text{Zr}, \text{Hf}$) leads to fluxional six-coordinate compounds that exhibit intermediate Bailar twist features in solution and in the solid state. Coordination of the 2,4-diimino-1,3-diazetidines to $\text{Zr}(\text{NMe}_2)_4$ results in a metal-mediated carbodiimide metathesis into two zirconium guanidinate complexes, which can be rationalized by a two-step reaction mechanism.



INTRODUCTION

Early transition metal coordination chemistry has been greatly impacted by the seminal report of the synthesis of 1,1-diaminoferrocene by Shafir and Arnold.¹ Since their contribution, the coordination chemistry of transition metal compounds bearing 1,1'-nitrogen disubstituted ferrocene containing ligands has grown extensively. Many of these ferrocene ligands can now be found in the literature: silyl amino derivatives,^{2,3} phosphinoamides,^{4,5} aryl amines synthesized by palladium cross-coupling reactions,⁶ azomethine type ligands,^{7–9} phosphazene based ones starting from 1,1'-diazidoferrocene¹⁰ and guanidines¹¹ to cite a few examples.

The ferrocene molecule has remarkable chemical stability allowing for easy derivatization (besides oxidizing agents) and makes a great tether for constructing pincer ligands (3.3 Å distance between cyclopentadienyl rings and ball bearing flexibility).^{12–16} It also imparts rigidity to structures which promotes good crystal packing while maintaining good solubility in common organic solvents. Additionally, ferrocene is an electrochemically active moiety allowing this class of compounds to be employed as redox switches to tune catalytic activity, as reported in recent literature examples.^{17–20}

In this study we sought to connect a missing link between ferrocene chemistry and nitrogen based heteroallylic ligands: the synthesis of 1,1'-dicarbodiimidoferrocene *proligands*. Although the related N,N' -diferrocenylcarbodiimide was reported as early as 1966,²¹ to the best of our knowledge the 1,1'-dicarbodiimidoferrocenes (Figure 1, I) have never been employed as *proligands* in coordination chemistry. Of related interest [3.3]-ferrocenophanes and the 2,4-diimino-1,3-azetidines have been exploited for ion sensing by various spectroscopic (NMR, UV–vis) and electrochemical means.^{22–24} More recently these kinds of ferrocenophanes

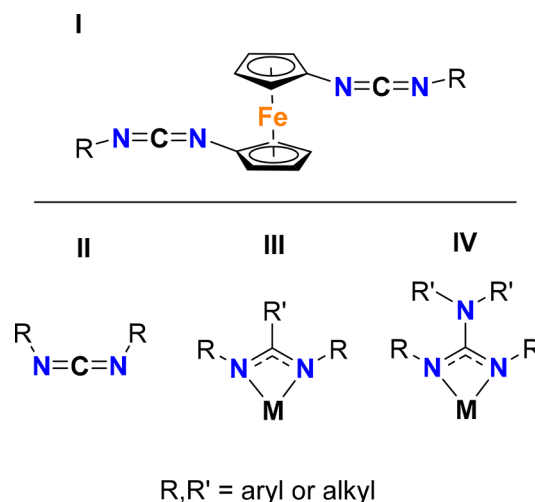


Figure 1. Top: 1,1'-dicarbodiimidoferrocene target compound of this study (I). Bottom: general structure of a carbodiimide (II), amidinate (III), and guanidinate (IV) binding motifs.

have been used as supporting structures for hosting diradicals.^{25,26} Carbodiimides (Figure 1, II) themselves find uses as *proligands* in inorganic chemistry due to their ability to bind a wide range of elements including the p-block elements (e.g., amidinato silylenes and heavier congeners,²⁷ likewise for boron²⁸) as tight bite angle supporting ligands in the form of amidinates (Figure 1, III) and the closely related guanidates (Figure 1, IV).^{29,30}

Received: May 21, 2019

Herein we report the straightforward synthesis of 4 new 1,1'-dicarbodiimidoferrocene based *proligands* (**1a–d**). The molecules and their equilibrium 2,4-diimino-1,3-diazetidines counterparts (**2a–d**) have been characterized by spectroscopic methods (NMR, FT-IR, UV–vis), solid state structures (XRD), and electrochemical studies (Cyclic voltammetry), and their coordination chemistry with group IV dimethylamido ferrocene complexes has been explored. Additionally, we describe new reactivity involving zirconium-mediated carbodiimide metathesis involving the 2,4-diimino-1,3-azetidine equilibrium products.

RESULTS AND DISCUSSION

Proligand Synthesis and Characterization. The 1,1'-dicarbodiimidoferrocene *proligands* were synthesized via a two-step one-pot procedure starting from 1,1'-diazidoferrocene. Using a suitable phosphine, the Staudinger phosphazene was generated *in situ*, followed by the addition of the corresponding isocyanate to obtain the desired carbodiimide plus phosphine oxide byproduct (Figure 2). This route was favored over other

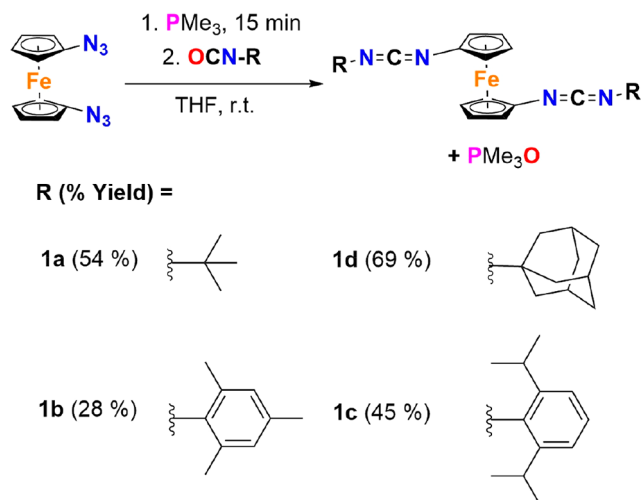


Figure 2. Synthetic procedure for the preparation of 1,1'-carbodiimidoferrocenes.

known methods to synthesize sterically hindered carbodiimides which involve oxidizing agents³¹ incompatible with ferrocene and prolonged heating in the presence of dehydrating agents^{32,33} to prevent side reactions.

Formation of the *tert*-butyl derivative (**1a**), which is a red oil at room temperature, was achieved using PPh_3 in refluxing THF. The synthesis of the mesityl (**1b**) and 2,6-diisopropyl derivatives (**1c**) (yellow solid and orange oil respectively) required the use of the less bulky PMe_3 for the reaction to proceed in acceptable yields. This method was also used for the synthesis of the adamantyl substituted *proligand* **1d** which is an orange solid at room temperature. Commercially available, more affordable, and easier to handle, PMe_3 solutions in toluene can be used instead of neat PMe_3 without affecting product yields.

The *proligands* (**1a–d**) were purified by column chromatography (silica gel) and recovered in excellent purity. If the separation is carried out in the air several grams can be isolated in one run. However, on a larger scale, oxidation occurs and a green tail is deposited on the column. We hypothesize that the

carbodiimide oxidizes to the corresponding urea in the presence of silica which readily binds to it and then further oxidizes to a green colored ferrocenium compound. Two-dimensional TLC confirmed that the recovered product remains unaltered upon passage through the column, although there is significant streaking left behind in the TLC plate (see Supporting Information (SI) Figure S1). The carbodiimide *proligands* should be stored under an inert atmosphere, as they will otherwise slowly oxidize in the air.

Interestingly, on storage at room temperature for 2 days the 2,6-diisopropyl derivative **1c** gave rise to a yellow solid which was identified as the 2,4-diimino-1,3-diazetidine intramolecular cycloaddition product **2c**. This behavior is known for other simple alkyl and aryl carbodiimides (*N,N'*-dicyclohexylcarbodiimide, *N,N'*-diisopropyl carbodiimide).^{34–36} Here the reaction is no doubt favored since the two carbodiimide moieties are linked and in close proximity forming exclusively the *E,E* isomer to minimize steric interactions of the bulky substituents. A recent computational study shows the ability of ferrocene to bend while in the eclipsed conformation thus allowing for intramolecular cyclizations like this to occur.³⁷ Prolonged storage of **1a** and **1d** neat and in C_6D_6 solutions shows no detectable conversion of the carbodiimide, whereas **1b** converts to **2b** in 42% yield in C_6D_6 solution after 38 days at room temperature but remains unaltered in the solid state. We were able to isolate the corresponding 2,4-diimino-1,3-diazetidines **2a**, **2b**, **2c**, and **2d** by conducting the reaction at $\sim 100^\circ\text{C}$ in toluene. Analysis of the reaction solutions showed incomplete conversion to the corresponding 2,4-diimino-1,3-diazetidines, although isolation and purification are straightforward due to the diminished solubility of the products in pentane. The relatively slow nature of these reactions allowed us to monitor the conversions over extended periods of time via NMR. These studies showed that in solution the carbodiimide and its cyclized product are in equilibrium (see reaction profiles SI S4). The equilibrium can be attained by starting from the 2,4-diimino-1,3-azetidines, and no other species are observed from further carbodiimide metathesis (e.g., no *N,N'*-di-*tert*-butylcarbodiimide was observed after heating **1a** even after extended periods of heating at 70°C in C_6D_6 solution).

The 2,4-diimino-1,3-diazetidine heterocycles **2a–d** exhibit distinct spectroscopic features compared to the parent carbodiimides. A hypsochromic shift of approximately 10 nm is observed in the UV–vis absorption maximum (see SI Figure S3) as well as a decrease in molar absorptivity in accordance with a lighter color of the bulk materials. The cyclization of the heterocycle prevents the free rotation along the ferrocene axis, and the pendant $-\text{R}$ groups become inequivalent and produce two diagnostic well resolved sets of signals in the ^1H NMR spectra. Additionally, the characteristic carbodiimide IR stretch at *ca.* 2100 cm^{-1} is no longer observed.

Repeated attempts to crystallize the oil **1c** at low temperature failed, and only the 2,4-diimino-1,3-diazetidine **2c** (SI Figure S4) and the corresponding bisurea could be crystallized. Attempts to obtain XRD quality crystals of the adamantyl substituted compounds **1d** and **2d** were also unsuccessful. However, we have been able to structurally characterize the *tert*-butyl derivatives **1a** and **2a** (Figure 3) and mesityl substituted analogs **1b** and **2b** (SI Figure S5). Condensation of the azetidine core causes the ferrocene moiety to bend with angles of 11° for **2a**, 13° for **2b**, and 11° for **2c** between the cyclopentadienyl planes. The cyclization

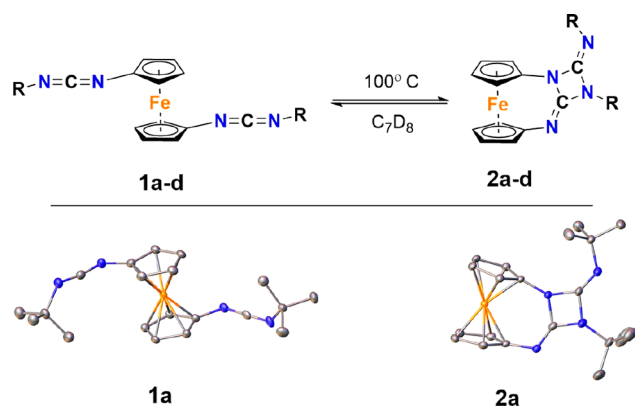


Figure 3. Top: Equilibrium established between the carbodiimide and 2,4-diimino-1,3-diazetidines species. Bottom: ORTEP diagrams portray the solid-state structures of **1a** and **2a**. Ellipsoids drawn at 50% probability; hydrogens have been omitted for clarity.

does not significantly shorten the distance between the cyclopentadienyl centroids remaining at ca. 3.3 Å. Crystallographic details for the single crystal X-ray studies are provided in the SI, and CIF files are available via the CCDC database.

Zirconium 1,1'-Bisguanidateferrocene Complexes: Synthesis and Characterization. Reaction of the *proligands* **1a–1d** with $\text{Zr}(\text{NMe}_2)_4$ in tetrahydrofuran or toluene at room temperature afforded the corresponding zirconium 1,1'-bisguanidateferrocene complexes (**3a–d**) in good yields. When left undisturbed the complexes simply crystallize from the reaction mixtures over a period of 4 to 24 h. This strategy permitted the isolation of relatively pure crystalline materials by decanting the supernatant, followed by repeated washing with solvent to remove unreacted starting materials. Purity was confirmed by both NMR and elemental analysis.

The initial NMR scale metalation studies of **1a** to yield **3a** using $\text{Zr}(\text{NMe}_2)_4$ showed a broad baseline in the ^1H NMR spectrum from 4.6 to 3.0 ppm and a *tert*-butyl resonance at 1.43 ppm. In order to rule out the generation of paramagnetic ferrocenium species, the product was isolated as a crystalline material and analyzed again giving rise to the same spectrum. A plausible explanation for the observed peak broadening is therefore not due to magnetic properties but caused by fluxional behavior of **3a**. The spectrum was acquired again at elevated temperature (90 °C), the broad peaks coalesced, and assignment of the observed resonances to a six-coordinate complex was made possible.

The observation that well resolved NMR spectra were not observed at room temperature for the alkyl substituted zirconium guanidinate complexes prompted us to synthesize the hafnium analogues (**4a–d**) and subject them to VT NMR studies. ^1H NMR spectra were recorded between –80 °C to 100 °C in increments of 20 °C. At low temperature the signals of the *tert*-butyl substituents are inequivalent (Figure 4), indicative of an octahedral compound with the guanidates in asymmetrical positions around the metal, whereas at high temperature an averaged signal was observed (Figure 4). These data are consistent with a Bailar twist rearrangement through a trigonal prismatic intermediate being the source of the peak broadening. This behavior is known for other group IV amidate and amidinate transition metal compounds and a recently reported zirconium ferrocene azomethine.^{38–40}

Interestingly, the mesityl and 2,6-diisopropyl substituted zirconium complexes (**3b**, **3c**) gave rise to interpretable ^1H

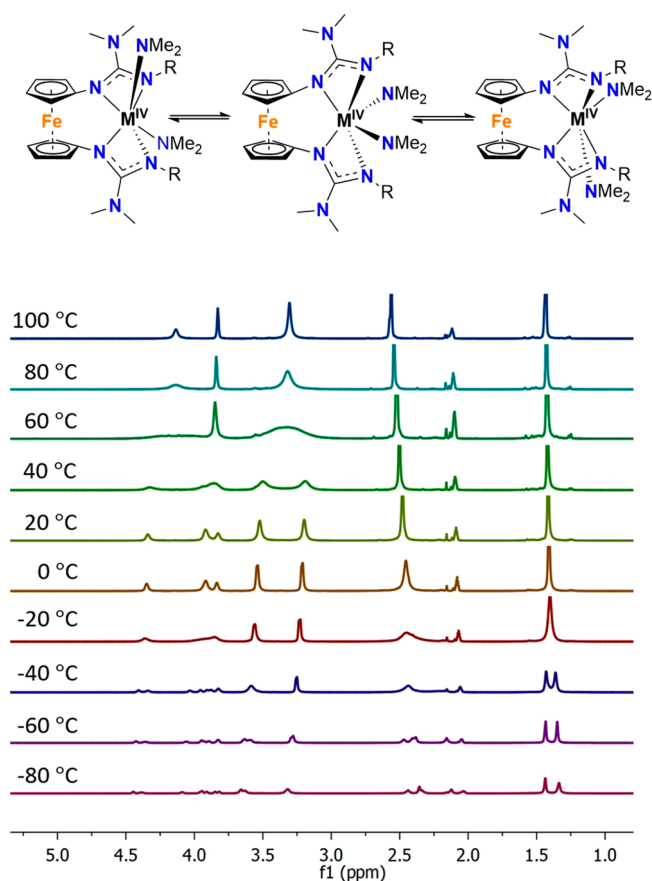


Figure 4. Bailar twist through a trigonal prismatic configuration. Below, VT- ^1H NMR of **4a** in C_7D_8 showing two distinct *tert*-butyl guanidinate resonances at low temperature (~ 1.5 ppm).

NMR spectra at room temperature, although some peak broadening is still present for the metal bound dimethylamide groups indicating that the exchange is not fully suppressed at room temperature. On the other hand, the adamantyl substituted compound **3d** resembled its **3a** counterpart showing extensive peak broadening.

The solid-state structures of the compounds confirmed the six-coordinate distorted octahedral geometry for the series of compounds. This is a conservative assignment of the geometry since the **3b** and **3c** structures appear to be more trigonal prismatic (Figure 5). This is not surprising given that the compounds exhibit Bailar twisting. The crystallographic parameters for **3a** and **3d** are distinctly different from those of **3b** and **3c**. Dimethylamides are strong ligands consequently exerting a significant thermodynamic trans effect on their trans ligand counterpart. Complexes **3a** and **3d** show significant lengthening (>0.1 Å) of the guanidinate nitrogen trans to the dimethylamides (see Figure 5). The angles between $\text{N}_{\text{trans}}-\text{Zr}-\text{NMe}_2$ are wider, approaching the ideal octahedral 180° angle. On the other hand, **3b** and **3c** are not as influenced by the trans effect with the guanidinate bond lengthening less than 0.05 Å. In these compounds the $\text{N}_{\text{trans}}-\text{Zr}-\text{NMe}_2$ angle has a more trigonal prismatic character (ideal, 132° ; **3b**: 140° , **3c** 145°). Finally, the angle formed between the dimethylamides, which are not influenced by the constriction of the ferrocene moiety, differ for the whole series ranging between 91° in **3a** to a 100° in **3c** (Ideal angles: Oh 90° , Trigonal prismatic 95°). We believe that in the *proligands* **3b** and **3c** there is more steric hindrance closer to the metal binding

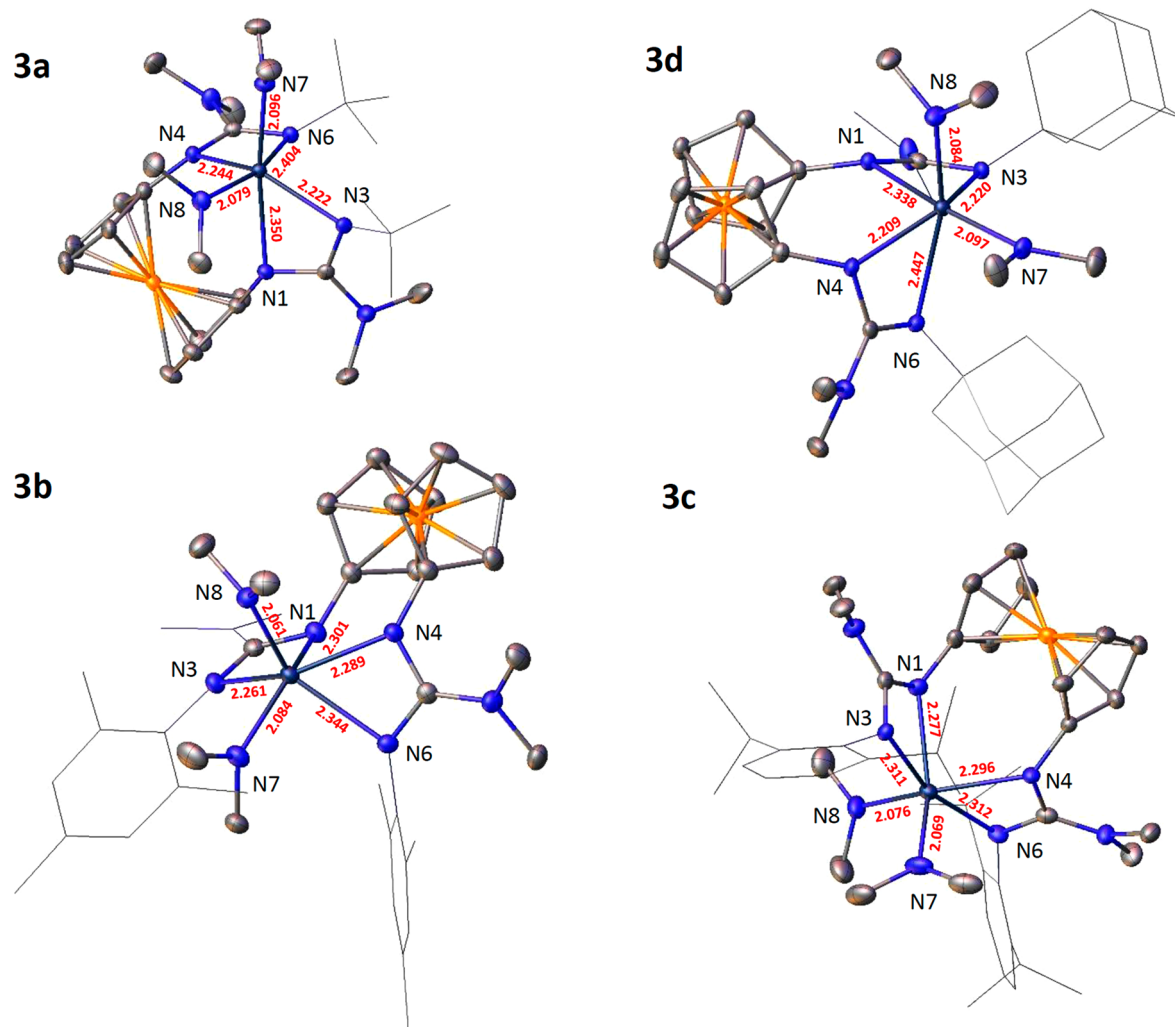


Figure 5. Solid state structures of compounds **3a–3d** drawn at the 50% ellipsoid probability. Hydrogens atoms removed for clarity. R groups are depicted as wireframe. Bond lengths are given in Å.

sphere since they both bear ortho substituted aryl rings, and this favors the trigonal pyramidal geometrical arrangement. Buried volume values and steric plots obtained with Sambvca2.0⁴¹ show increased substituent interactions in **3b** and **3c** (see SI for plots). Bite angles of the guanidates are not affected by the ferrocene tether. The hafnium analogues are isostructural due to the similar radius of zirconium(IV) and hafnium(IV); the structural parameters show an identical trend.⁴²

We have explored reactions of **3a–d** with PMe_3 and N,N -dimethylaminopyridine, since the addition of a small two-electron donor would give the complexes an 18 electron count and might stabilize a seven-coordinate pentagonal bipyramidal geometry. However, no incorporation of a neutral donor was observed when an excess was added to the reaction mixture before the addition of $\text{Zr}(\text{NMe}_2)_4$ to the carbodiimido ligands.

Reactivity of 2,4-Diimino-1,3-diazetidines with $\text{Zr}(\text{NMe}_2)_4$. We have also studied the Zr metalation reactions of the 2,4-diimino-1,3-diazetidines in order to determine if they could act as *proligands*. The reaction of $\text{Zr}(\text{NMe}_2)_4$ with the carbodiimides **1a** and **1b** to afford **3a** and **3b** occurs rapidly, in under 10 min, as judged by NMR. Addition of the metal source causes an immediate darkening of the orange proligand solution. We hypothesized that this fast guanidinate formation

would result in eventual depletion of the 2,4-diimino-1,3-diazetidines through the carbodiimide equilibrium.

In contrast, the reaction between **2b** and a slight excess of $\text{Zr}(\text{NMe}_2)_4$ at room temperature in C_6D_6 remains unchanged after 24 h and the solution remains yellow in color. Heating to 75 °C results in a reaction which is complete after 68 h as judged by the consumption of $\text{Zr}(\text{NMe}_2)_4$ and gives rise to a complex mixture of species which we have identified. The peak assignments, aided by 2D NMR experiments, revealed a mixture composed of traces of unreacted **2b**, traces of **3b** produced by the reverse equilibrium reaction, and two major zirconium bearing components species **5** and **7** with some traces of guanidinate complex **9** (Figure 6). A similar behavior is observed in the reaction of **2a** with $\text{Zr}(\text{NMe}_2)_4$. Bis-(guanidinate) complexes **3a** and **3b** are thermodynamically stable at 75 °C in C_6D_6 for weeks and do not give rise to any further rearrangement.

Attempts to separate this reaction mixture were unsuccessful. Evaporating the solvent of the crude mixture and redissolving the residue in hexanes allowed only the separation of minor quantities of **9** (likely produced from the excess $\text{Zr}(\text{NMe}_2)_4$ available when **1a** is generated). Slow evaporation of the hexane solution afforded crystals of **2b** and a gooey residue containing a mixture of **2b**, **5**, and **7**. Compound **7** was

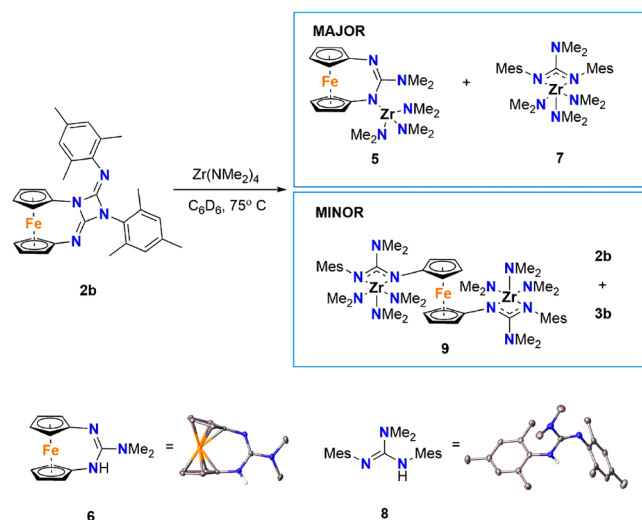
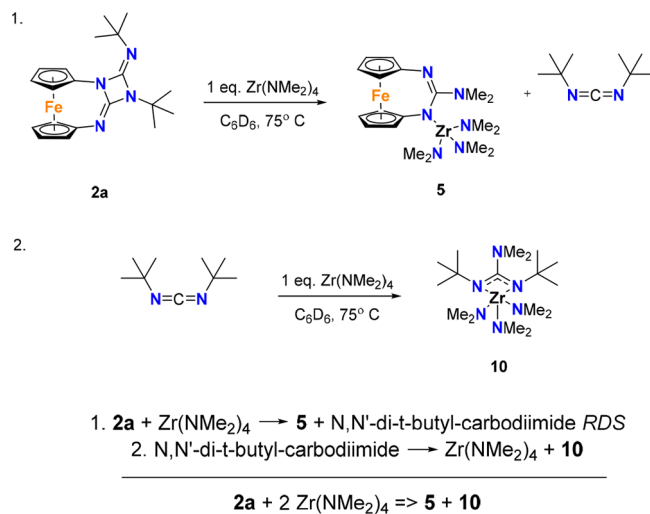


Figure 6. Species identified in the reaction of 1 equiv of **2b** with 2.1 equiv of Zr(NMe₂)₄.

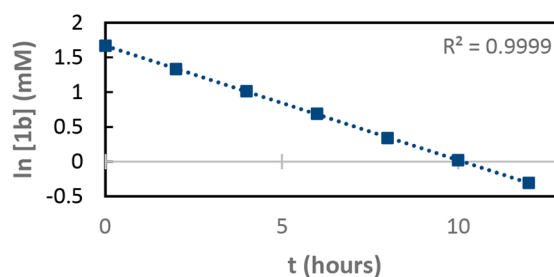
independently prepared from *N,N'*-dimesityl carbodiimide and Zr(NMe₂)₄, and **5** was prepared from recovered ligand **6** and Zr(NMe₂)₄ for unambiguous identification. The NMR resonances of the independently synthesized samples correspond well with the observed reaction products. Additionally, the LC-MS of the crude mixture reaction showed the presence of free guanidines **6** and **8**.

A plausible explanation for these results begins with a new reaction pathway via coordination of the diimine lone pair to Zr(NMe₂)₄ (Figure 7). In order to gather more information about the unusual transformations taking place in the reactions of the azetidines **2a** and **2b** with Zr(NMe₂)₄ (Figures 6, 7), we obtained kinetic data for the thermally activated process. We employed pseudo-first-order conditions⁴³ using **2a** with high concentrations of Zr(NMe₂)₄ which also reduces reaction times and thus minimizes side generation of **3a**. The rate of reaction was found to be first-order for both **2a** and Zr(NMe₂)₄ [rate = *k*[**2a**][Zr(NMe₂)₄]. A two-step reaction mechanism can be postulated (Figure 7) comprised of a slow rate-determining step of the reaction between **2a** and 1 equiv of Zr(NMe₂)₄ to generate **5**. This step also produces an equivalent of *N,N'*-di-*tert*-butylcarbodiimide that rapidly reacts with an additional equivalent of Zr(NMe₂)₄ to form **10**, the analog of **7**. This is also consistent with the rapid reactions observed between independently synthesized guanidinate compounds. Steric plots of **2a** and **2b** show less hindrance at the ferrocene diimine site (vs the ring bound diamine) suggesting that steric factors play a role in the initial formation of **5**.

Electrochemistry. Electrochemical studies of ferrocene-containing compounds are now well-known. We studied the electrochemical behavior of the carbodiimide *proligands*, the 2,4-diimino-1,3-diazetidines, and the metal complexes (see SI for details). Carbodiimides **1a–d** show a reversible freely diffusing redox couple assigned to the one-electron oxidation of the ferrocene moiety in 0.1 M [NBu₄][PF₆] in dichloromethane. At higher potentials an irreversible oxidation event occurs assigned to the oxidation of the carbodiimide C=N bonds as previously established.^{11,44–46} Azetidines **2a–d** also have a one-electron reversible oxidation of the ferrocene couple shifted to more oxidizing potentials followed again by another irreversible oxidation event occurring at the 2,4-



First Order Dependence on **2a**



First Order Dependence on Zr(NMe₂)₄

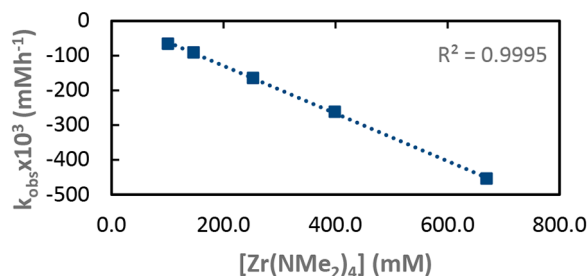


Figure 7. Proposed mechanism for the reaction of **2a/2b** with Zr(NMe₂)₄. The conversion plots reveal first-order dependency for both 2,4-diimino-1,3-azetidine and Zr(NMe₂)₄. Additional details regarding kinetics can be found in the SI.

diimino-1,3-diazetidines. The increase in the potential is attributed to the electron-withdrawing character of the 2,4-diimino-1,3-azetidine heterocycle (Figure 8). The study of compound **6** in 0.1 M [NBu₄][PF₆] tetrahydrofuran solution revealed an irreversible oxidation at 544 mV likely occurring at the strained guanidine followed by a reversible electrochemical event assigned to the ferrocenium couple at 911 mV (see SI S22).

For the Zr complexes our studies were limited to **3a** and **3b** as representative examples of alkyl and aryl substituted ligand metal complexes. The voltammogram for **3a** in 0.1 M [NBu₄][PF₆] tetrahydrofuran has a freely diffusing reversible event occurring at -720 mV assigned to the ligand Fc/Fc⁺ and a quasi-reversible event at -338 mV likely occurring at the guanidinate ligand. On the other hand, the voltammogram for

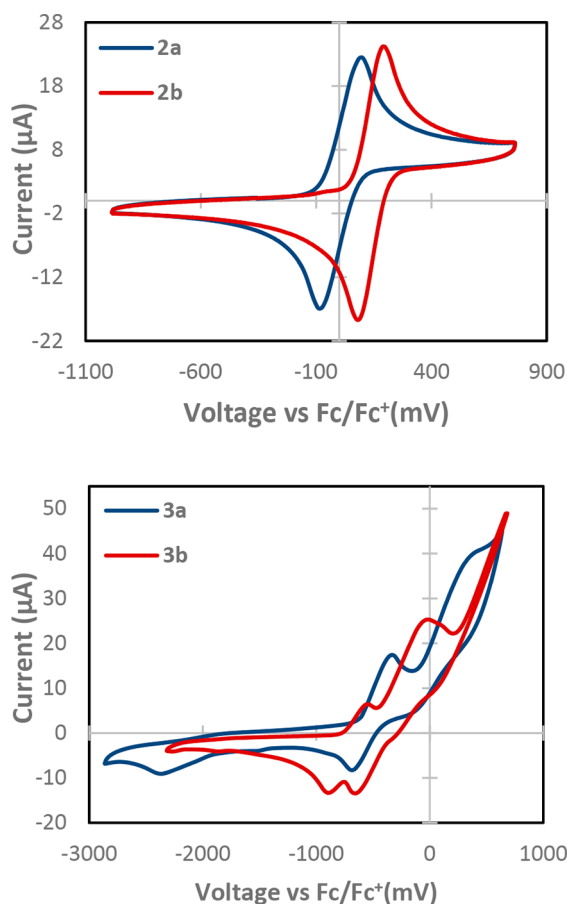


Figure 8. Top: Cyclic voltammogram of representative carbodiimide **2a** and 2,4-diimino-1,3-diazetidone **2b**. Bottom: Cyclic voltammogram of metal complexes **3a** and **3b**.

3b shows a quasi-reversible event at -500 mV assigned to the tether Fc/Fc^+ occurring at the electrode interface as revealed by the scan rate dependency. At higher potential (430 mV) an irreversible event is observed involving the decomposition of the complex through the guanidinate (Figure 8).

CONCLUSIONS

In summary, a new family of disubstituted ferrocene compounds has been synthesized and studied. We have shown that 1,1'-dicarbodiimidoferrocenes can be employed as heteroallylic *proligands* by isolation of their guanidinate early transition metal complexes. The 1,1'-dicarbodiimidoferrocenes are in equilibrium with their 2,4-diimino-1,3-diazetidone counterparts which, in the presence of $\text{Zr}(\text{NMe}_2)_4$, favor carbodiimide metathesis forming two separate zirconium-bearing guanidinate species.

EXPERIMENTAL SECTION

Unless otherwise stated manipulations were carried out using standard Schlenk techniques or in a VAC HE-63P nitrogen-filled glovebox. Dry degassed solvent was obtained from the Innovative Technologies Solvent Purification system and stored over 4 Å molecular sieves prior to use. Deuterated benzene and toluene were distilled from sodium/benzophenone ketyl and stored over 4 Å molecular sieves in Teflon valved flasks. NMR spectroscopy was performed on an Agilent MR 400, Bruker Avance III HD 500, or a Varian VNMRs 600 and processed using Mestrenova. NMR spectra were acquired at room temperature unless otherwise specified. IR spectra were obtained on a Nicolet iSSO FT-IR spectrometer using

attenuated total reflectance (ATR). Electrochemical experiments were performed on a Pine Research Instrumentation Inc. WaveNow potentiostat, and potentials are referenced to the ferrocene/ferrocenium couple. Mass spectrometry data were provided by the UT Austin Mass Spectrometry Facility. X-ray crystallography was performed in the The University of Texas—X-ray Diffraction Laboratory. Elemental analysis (C, H, N) were performed by Midwest Microlab Inc. Indianapolis, IN. 1,1'-Diazidoferrocene was prepared according to the method reported by Arnold.¹ **Caution:** *Necessary precautions should be taken for the handling of this potentially explosive compound.* Mesityl isocyanate and 2,6-diisopropylisocyanate were prepared from the corresponding amine and di-*tert*-butyl dicarbonate.⁴⁷ 1-Adamantyl isocyanate was prepared using triphosgene starting from 1-adamantylammonium chloride. Detailed multi-gram procedures are given in the SI.

1,1'-Di-*tert*-butylcarbodiimidoferrocene (1a). 1,1'-Diazidoferrocene (2.9 g, 10.8 mmol) was dissolved in tetrahydrofuran (150 mL), triphenylphosphine (6.25 g, 23.8 mmol) was added, and the mixture was stirred for 3 h. Neat *tert*-butyl isocyanate (2.5 mL, 22.1 mmol) was then added, and the red suspension was refluxed for 14 h until it turned into a clear burnt orange colored solution. Solvent was removed under vacuum, and the oily residue was extracted with pentane (50 mL) and filtered to remove the bulk of PPh_3O which was washed with pentane (2×25 mL). Solvent was removed under reduced pressure, and the residue was purified by silica gel column chromatography using ethyl acetate/hexanes (3:97, $R_f = 0.33$) affording the title compound as a red oil. Yield (2.22 g, 54%). Alternatively, PPh_3 can be substituted by tri-*n*-butyl phosphine, and the reaction with isocyanate proceeds at room temperature in this case. Even though purification can be performed in air, the product should be stored under an inert atmosphere. ^1H NMR (500 MHz, Benzene- d_6) δ 4.30 (t, $J = 1.9$ Hz, 4H, Cp-H), 3.92 (t, $J = 1.9$ Hz, 4H, Cp-H), 1.22 (s, 18H, $-\text{C}(\text{CH}_3)_3$). ^{13}C NMR (126 MHz, Benzene- d_6) δ 137.8 ($-\text{N}=\text{C}=\text{N}-$), 98.5 (Cp-C-N), 66.7 (Cp-CH), 65.1 (Cp-CH), 56.3 ($-\text{C}(\text{CH}_3)_3$), 31.5 ($-\text{C}(\text{CH}_3)_3$). FT-IR (ATR, cm^{-1}) 2970, 2193, 2112, 1497, 1460, 1393, 1365, 1237, 1198, 1022, 919, 848, 814, 724, 693, 597, 533, 491, 442. HR-MS (ESI) m/z 399.1449 [Calculated for $\text{C}_{20}\text{H}_{26}\text{N}_4\text{FeNa}^+$ 399.1446].

1,1'-Dimesitylcarbodiimidoferrocene (1b). 1,1'-Diazidoferrocene (1 g, 3.73 mmol) was dissolved in tetrahydrofuran (30 mL), and PMe_3 (0.8 mL, 7.84 mmol) was added dropwise and stirred for 15 min until nitrogen evolution ceased. Solid mesitylisocyanate (1.26 g, 7.84 mmol) was then added, and the mixture was stirred for 18 h at room temperature. The solvent was evaporated under reduced pressure, the residue was extracted with pentane (3×15 mL) followed by filtering to remove PMe_3O , and the solvent was evaporated again. The resulting oily residue was purified by silica column chromatography with ethyl acetate/hexanes (3:97, $R_f = 0.26$). The title compound was obtained as a yellow solid. Yield (530 mg, 28%). ^1H NMR (500 MHz, Chloroform- d) δ 6.83 (s, 4H, Aryl-H), 4.34 (t, $J = 1.9$ Hz, 4H, Cp-H), 4.10 (t, $J = 1.9$ Hz, 4H, Cp-H), 2.33 (s, 12H, Aryl- CH_3), 2.24 (s, 6H, Aryl- CH_3). ^{13}C NMR (126 MHz, Chloroform- d) δ 134.6 (C_q), 132.5 (C_q), 132.4 (C_q), 132.2 (C_q), 128.8 (Aryl-CH), 97.1 (Cp-C-N), 66.7 (Cp-CH), 64.8 (Cp-CH), 20.8 (Aryl- CH_3), 18.9 (Aryl- CH_3). FT-IR (ATR, cm^{-1}) 2915, 2856, 2132, 2105, 1581, 1525, 1472, 1432, 1366, 1223, 1098, 1020, 955, 936, 915, 851, 814, 724, 669, 621, 593, 543, 523, 490. Melting Point: 87–88 °C. HR-MS (ESI) m/z 503.1887 [Calculated for $\text{C}_{30}\text{H}_{31}\text{N}_4\text{Fe}^+$ 503.1893].

1,1'-Di(2,6-diisopropylphenyl)carbodiimidoferrocene (1c). 1,1'-Diazidoferrocene (1 g, 3.73 mmol) was dissolved in tetrahydrofuran (25 mL), and PMe_3 (0.8 mL, 7.84 mmol) was added dropwise and stirred for 15 min until nitrogen evolution ceased. 2,6-Diisopropylisocyanate (1.59 g, 7.84 mmol) was added as a solution in toluene (10 mL), and the mixture was stirred for 18 h at room temperature. The solvent was evaporated under reduced pressure, the residue was extracted with pentane (3×15 mL) followed by filtering to remove PMe_3O , and the solvent was evaporated again. The oily residue was purified by silica column chromatography using ethyl acetate/hexanes (2:98, $R_f = 0.28$). The title compound was isolated as an orange colored oil. Yield (979 mg, 45%). ^1H NMR (500 MHz,

Chloroform-*d*) δ 7.13 (m, 6H, Aryl-*H*), 4.33 (t, J = 1.9 Hz, 4H, Cp-*H*), 4.10 (t, J = 1.9 Hz, 4H, Cp-*H*), 3.38 (hept, J = 6.9 Hz, 4H, Aryl-CH(CH₃)₂), 1.28 (d, J = 6.9 Hz, 24H, Aryl-CH(CH₃)₂). ¹³C NMR (126 MHz, Chloroform-*d*) δ 142.4 (–N=C=N–), 132.5 (C_q), 130.2 (C_q), 125.5 (Aryl-CH), 123.3 (Aryl-CH), 97.1 (Cp-C-N), 66.9 (Cp-CH), 64.9 (Cp-CH), 29.2 (Aryl-CH(CH₃)₂), 23.2 (Aryl-CH(CH₃)₂). FT-IR (ATR, cm^{–1}) 2960, 2868, 2136, 1588, 1526, 1437, 1383, 1363, 1322, 1256, 1246, 1212, 1181, 1144, 1106, 1083, 1059, 1042, 1020, 934, 917, 807, 795, 748, 666, 620, 592, 545, 516, 491. HR-MS (ESI) m/z 587.2822 [Calculated for C₃₆H₄₃N₄Fe⁺ 587.2832].

1,1'-Diadamantylcarbodiimidoferrocene (1d). 1,1'-Diazidoferrocene (3 g, 11.2 mmol) was dissolved in tetrahydrofuran (75 mL), and PMe₃ (1 M in toluene, 22.5 mL) was added dropwise and stirred for 15 min until nitrogen evolution ceased. Adamantylisocyanate (4 g, 22.6 mmol) was added as a solution in tetrahydrofuran (20 mL). The mixture was stirred for 4 h at room temperature. The solvent was evaporated under reduced pressure, and the residue was extracted with a 50:50 ether/pentane mixture (3 × 30 mL). The combined extracts were filtered to remove the bulk of PMe₃O. The filtrate was dry loaded in diatomaceous earth and purified by silica column chromatography using ethyl acetate/hexanes (2:98, R_f = 0.22). After evaporation of the solvent the title compound was obtained as an orange colored solid. Yield (4.12 g, 69%). ¹H NMR (500 MHz, Benzene-*d*₆) δ 4.38 (t, J = 1.9 Hz, 4H, Cp-*H*), 3.98 (t, J = 1.9 Hz, 4H, Cp-*H*), 1.92–1.86 (m, 18H, CH₂+CH), 1.49–1–43 (m, 12H, –CH₂–). ¹³C NMR (126 MHz, Benzene-*d*₆) δ 138.3 (–N=C=N–), 98.8 (Cp-C-N), 66.8 (Cp-CH), 65.2 (Cp-CH), 56.8 (N-C-Adamantyl), 45.3 (–CH₂–), 36.1 (–CH₂–), 30.2 (–CH–). FT-IR (ATR, cm^{–1}) 2902, 2848, 2093, 1493, 1451, 1353, 1303, 1265, 1192, 1101, 1062, 1019, 972, 920, 880, 811, 773, 717, 694, 619, 550, 483, 403. Melting Point: >283 °C (dec.). HR-MS (ESI) m/z 557.2337 [Calculated for C₃₂H₃₈N₄FeNa⁺ 557.2339].

2,4-Diimino-1,3-diazetidene (2a). A Teflon valved Schlenk tube was charged with a solution of **1a** (130 mg, 0.34 mmol) in toluene (5 mL) and heated at 110 °C for 48 h. Conversion to the azetidene was determined to be 32% by ¹H NMR. The solvent was evaporated under vacuum, and the resulting semisolid was washed with pentane (3 × 1 mL) to eliminate unreacted **1a** and dried to afford the title compound as a bright yellow solid. Isolated yield (24 mg, 18%). ¹H NMR (500 MHz, Benzene-*d*₆) δ 3.98–3.96 (m, 4H, Cp-*H*), 3.89 (t, J = 1.9 Hz, 2H, Cp-*H*), 3.83 (t, J = 1.9 Hz, 2H, Cp-*H*), 1.66 (s, 9H, –C(CH₃)₃), 1.38 (s, 9H). ¹³C NMR (126 MHz, Benzene-*d*₆) δ 161.3 (C_q), 140.9 (C_q), 111.7 (Cp-C-N), 83.0 (Cp-C-N), 71.9 (Cp-CH), 70.2 (Cp-CH), 67.6 (Cp-CH), 65.9 (Cp-CH), 55.6 (–C(CH₃)₃), 53.2 (–C(CH₃)₃), 32.1 (–C(CH₃)₃), 28.5 (–C(CH₃)₃). FT-IR (ATR, cm^{–1}) 3102, 3082, 2961, 2926, 2251, 1789, 1660, 1478, 1352, 1456, 1389, 1352, 1263, 1233, 1210, 1127, 1089, 1056, 1030, 1021, 940, 854, 875, 842, 816, 802, 752, 715, 679, 653, 606, 524, 495, 458, 436. Melting Point: 178–179 °C HR-MS (ESI) m/z 379.1589 [Calculated for C₂₀H₂₇N₄Fe⁺ 379.1580].

2,4-Diimino-1,3-diazetidene (2b). A Teflon valved Schlenk tube was charged with compound **1b** (115 mg, 0.23 mmol) in toluene (5 mL) and heated at 100 °C for 18 h. The solvent was evaporated under reduced pressure to afford a yellow oil. Addition of pentane (3 mL) induces precipitation of the product which was isolated by filtration and washed with additional pentane (3 mL). The title compound was obtained as an orange powder. Yield (51 mg, 44%). ¹H NMR (500 MHz, Chloroform-*d*) δ 6.93 (s, 2H, Aryl-*H*), 6.63 (s, 2H, Aryl-*H*), 4.20–4.15 (m, 2H, Cp-*H*), 4.09 (t, J = 1.9 Hz, 2H, Cp-*H*), 4.01 (m, 4H, Cp-*H*), 2.45 (s, 6H, Aryl-CH₃), 2.28 (s, 3H, Aryl-CH₃), 2.17 (s, 6H, Aryl-CH₃), 2.10 (s, 3H, Aryl-CH₃). ¹³C NMR (126 MHz, Chloroform-*d*) δ 159.5 (C_q), 144.2 (C_q), 139.8 (C_q), 138.7 (C_q), 137.4 (C_q), 132.3 (C_q), 129.2 (Aryl-CH), 128.4 (C_q), 128.0 (Aryl-CH), 127.6 (C_q), 109.8 (Cp-C-N), 79.5 (Cp-C-N), 70.6 (Cp-CH), 69.7 (Cp-CH), 67.00 (Cp-CH), 65.7 (Cp-CH), 21.1 (Aryl-CH₃), 20.7 (Aryl-CH₃), 18.4 (Aryl-CH₃), 18.3 (Aryl-CH₃). FT-IR (ATR, cm^{–1}) 3086, 2914, 1789, 1669, 1609, 1578, 1474, 1437, 1394, 1374, 1338, 1302, 1225, 1194, 1158, 1064, 1038, 1022, 1002, 954, 927, 913, 867, 852, 834, 819, 806, n774, 731, 712, 666, 613, 590, 563, 542, 513, 499,

489, 473, 447, 423. Melting Point: 174–175 °C. HR-MS (ESI) m/z 503.1886 [Calculated for C₃₀H₃₁N₄Fe⁺ 503.1893].

2,4-Diimino-1,3-diazetidene (2c). Proligand **1c** spontaneously converts to the corresponding azetidene. A vial containing neat **1c** oil develops visible solid azetidene after only 2 days from isolation. Here, we describe a simple purification method. A two-week-old vial containing a dark semi solid of **1c** (89 mg, 0.15 mmol) was supplemented with pentane (1 mL) and crushed to afford a yellow solid which was isolated by filtration and washed with additional pentane (2 × 1 mL). Yield of pale yellow solid (34 mg, 38%). ¹H NMR (500 MHz, Chloroform-*d*) δ 7.39 (t, J = 7.7 Hz, 1H, Aryl-*H*), 7.26 (d, J = 7.8 Hz, 2H, Aryl-*H*), 6.93–6.87 (m, 3H, Aryl-*H*), 4.14 (t, J = 2.0 Hz, 2H, Cp-*H*), 4.06 (t, J = 1.9 Hz, 2H, Cp-*H*), 4.00 (t, J = 1.9 Hz, 2H, Cp-*H*), 3.98 (t, J = 1.9 Hz, 2H, Cp-*H*), 3.38 (hept, J = 6.9 Hz, 2H, Aryl-CH(CH₃)₂), 3.17 (hept, J = 6.9 Hz, 2H, Aryl-CH(CH₃)₂), 1.40 (d, J = 6.9 Hz, 6H, Aryl-CH(CH₃)₂), 1.36 (d, J = 6.9 Hz, 6H, Aryl-CH(CH₃)₂), 1.25–1.13 (br, 12H, Aryl-CH(CH₃)₂). ¹³C NMR (126 MHz, Chloroform-*d*) δ 160.6 (C_q), 148.9 (C_q), 144.1 (C_q), 140.1 (C_q), 139.1 (C_q), 129.9 (Aryl-CH), 127.2 (C_q), 123.9 (Aryl-CH), 123.8 (Aryl-CH), 122.2 (Aryl-CH), 109.7 (Cp-C-N), 79.8 (Cp-C-N), 71.2 (Cp-CH), 69.5 (Cp-CH), 67.0 (Cp-CH), 65.7 (Cp-CH), 29.5 (Aryl-CH(CH₃)₂), 28.6 (Aryl-CH(CH₃)₂), 24.3 (Aryl-CH(CH₃)₂), 23.7 (Aryl-CH(CH₃)₂), 23.1 (br, Aryl-CH(CH₃)₂). FT-IR (ATR, cm^{–1}) 2961, 2869, 1790, 1678, 1588, 1447, 1402, 1383, 1374, 1336, 1255, 1240, 1205, 1174, 1108, 1061, 1041, 1025, 1004, 937, 924, 828, 808, 795, 784, 756, 740, 723, 692, 665, 614, 516, 498, 428, 405. Melting Point: 169–170 °C. HR-MS (ESI) m/z 587.2832 [Calculated for C₃₆H₄₃N₄Fe⁺ 587.2832].

2,4-Diimino-1,3-diazetidene (2d). A Teflon valved Schlenk tube was charged with a solution of **1d** (115 mg, 0.21 mmol) in toluene (5 mL) and heated at 100 °C for 65 h. Conversion was determined to be 19% by ¹H NMR. The toluene was evaporated under reduced pressure and the resulting solid was washed in the flask with pentane (3 × 5 mL) to remove the starting carbodiimide affording 90% pure material. Although impractical due to the lipophilicity of both **1d** and **2d**, higher purity material can be recovered by reversed phase preparative HPLC. Yield of light-yellow powder (10 mg, 8%). ¹H NMR (500 MHz, Benzene-*d*₆) δ 4.02 (dt, J = 5.7, 1.9 Hz, 4H, Cp-*H*), 3.90 (t, J = 1.9 Hz, 2H, Cp-*H*), 3.83 (t, J = 1.9 Hz, 2H, Cp-*H*), 2.64 (d, J = 3.0 Hz, 6H, –CH₂–), 2.15 (d, J = 2.9 Hz, 6H, –CH₂–), 2.04–1.96 (m, 6H, –CH–), 1.69–1.64 (m, 3H, –CH₂–), 1.56–1.50 (m, 9H, –CH₂–). ¹³C NMR (126 MHz, Benzene-*d*₆) δ 160.8 (C_q), 140.4 (C_q), 111.8 (Cp-C-N), 83.5 (Cp-C-N), 71.9 (Cp-CH), 70.2 (Cp-CH), 67.6 (Cp-CH), 65.9 (Cp-CH), 56.6 (N-C-Adamantyl), 53.9 (N-C-Adamantyl), 45.1 (–CH₂–), 41.5 (–CH₂–), 36.7 (–CH₂–), 36.6 (–CH₂–), 30.3 (–CH–), 29.9 (–CH–). FT-IR (ATR, cm^{–1}) 2904, 2851, 1790, 1669, 1479, 1453, 1358, 1344, 1326, 1306, 1262, 1242, 1187, 1099, 1056, 1040, 1023, 975, 934, 926, 883, 848, 808, 798, 775, 758, 739, 714, 694, 670, 628, 598, 558, 530, 520, 500, 461, 422. Melting Point: >283 °C (dec.). HR-MS (ESI) m/z 535.2521 [Calculated for C₃₂H₃₉N₄Fe⁺ 535.2519].

Complex (3a) [C₂₈H₅₀FeN₈Zr]. In a vial proligand **1a** (95 mg, 0.25 mmol) was dissolved in tetrahydrofuran (0.35 mL), and solid Zr(NMe₂)₄ (70 mg, 0.25 mmol) was added to the orange colored solution and shaken until homogeneous. After 4 h, complex **3a** deposited as orange crystalline needles. The supernatant was removed, and the crystals were washed with additional tetrahydrofuran (0.1 mL) and then dried under vacuum to obtain **3a**. Yield (84 mg, 52%). ¹H NMR (600 MHz, Toluene-*d*₈, 90 °C) δ 4.12 (q, J = 2.2 Hz, 4H, Cp-*H*), 3.82 (q, J = 2.1 Hz, 4H, Cp-*H*), 3.20 (br, 12H, Zr–N(CH₃)₂), 2.52 (d, 12H, guanidinate-N(CH₃)₂), 1.40 (d, 18H, –C(CH₃)₃). ¹³C NMR (151 MHz, Toluene-*d*₈, 90 °C) δ 170.0 (br, guanidinate-C), 107.0 (Cp-C-N), 64.2 (Cp-CH), 63.8 (br, Cp-CH), 53.6 (–C(CH₃)₃), 45.4 (Zr–N(CH₃)₂), 40.8 (guanidinate-N(CH₃)₂), 31.9 (–C(CH₃)₃). FT-IR (ATR, cm^{–1}) 3096, 3078, 2963, 2847, 2801, 2753, 1603, 1526, 1475, 1456, 1388, 1354, 1282, 1234, 1134, 1198, 1183, 1066, 1053, 1010, 954, 939, 835, 786, 762, 724, 684, 636, 617, 509, 485, 434. Melting Point: 204 °C. Elemental Analysis Anal. Found: C, 51.76; H, 7.61; N, 16.53. Calcd [C₂₈H₅₀FeN₈Zr]: C, 52.07; H, 7.80; N, 17.35.

Complex (3b) [C₃₈H₅₄FeN₈Zr]. Proligand **1b** (100 mg, 0.2 mmol) was dissolved in hexanes (0.25 mL), supplemented with Zr(NMe₂)₄ (54 mg, 0.2 mmol), and gently shaken until homogeneous. After 1 day, crystalline residue deposited in the bottom of the vial. The supernatant was removed, and the orange colored crystals were washed with hexanes (3 × 0.1 mL) and dried under vacuum to obtain **3b**. Yield (56 mg, 37%). ¹H NMR (400 MHz, Toluene-*d*₈) δ 6.73 (s, 4H, Aryl-*H*), 4.34 (t, *J* = 1.9 Hz, 4H, Cp-*H*), 3.91–3.84 (t, *J* = 1.9 Hz, 4H, Cp-*H*), 2.85 (s, 12H, Zr-N(CH₃)₂), 2.33 (s, 12H, Aryl-CH₃), 2.17 (br, 12H, guanidinate-N(CH₃)₂), 2.14 (br, 6H, Aryl-CH₃). ¹³C NMR (101 MHz, Toluene-*d*₈) δ 168.8 (guanidinate-C), 144.6 (C_q), 137.5 (C_q), 132.5 (C_q), 131.6 (C_q), 129.2 (Aryl-CH), 109.5 (Cp-C-N), 64.0 (Cp-CH), 64.0 (Cp-CH), 44.3 (Zr-N(CH₃)₂), 38.3 (guanidinate-N(CH₃)₂), 20.9 (Aryl-CH₃), 19.2 (Aryl-CH₃). FT-IR (ATR, cm⁻¹) 3088, 2912, 2855, 1621, 1600, 1532, 1472, 1393, 1372, 1273, 1198, 1144, 1159, 1022, 1003, 941, 880, 855, 814, 798, 762, 737, 683, 629, 582, 517, 490. Melting Point: 274 °C. Elemental Analysis Anal. Found: C, 59.49; H, 7.01; N, 14.41. Calcd [C₃₈H₅₄FeN₈Zr]: C, 59.28; H, 7.07; N, 14.55.

Complex (3c) [C₄₄H₆₆FeN₈Zr]. In a vial, proligand **1c** (100 mg, 0.17 mmol) was dissolved in hexanes (0.2 mL). Solid Zr(NMe₂)₄ (46 mg, 0.17 mmol) was added, and the mixture was left to stand overnight upon which a crystalline residue was obtained. The supernatant was removed, and the crystals were washed with hexanes (3 × 0.1 mL) and dried under vacuum to obtain **3c**. Yield (76 mg, 47%). ¹H NMR (600 MHz, Toluene-*d*₈, 90 °C) δ 4.24–4.18 (m, 4H, Cp-*H*), 3.92–3.87 (m, 4H, Cp-*H*), 3.65 (hept, *J* = 1.8 Hz, 4H, Aryl-CH(CH₃)₂), 2.81–2.80 (m, 12H, Zr-N(CH₃)₂), 2.35 (br, 12H, guanidinate-N(CH₃)₂), 1.33 (m, 24H, Aryl-CH(CH₃)₂). ¹³C NMR (151 MHz, Toluene-*d*₈, 90 °C) δ 168.2 (guanidinate-C), 143.9 (C_q), 143.5 (C_q), 125.2 (Aryl-CH), 123.8 (Aryl-CH), 111.4 (Cp-C-N), 64.3 (Cp-CH), 62.7 (Cp-CH), 44.4 (Zr-N(CH₃)₂), 39.7 (guanidinate-N(CH₃)₂), 28.0 (Aryl-CH(CH₃)₂), 24.9 (Aryl-CH(CH₃)₂), 24.9 (Aryl-CH(CH₃)₂). FT-IR (ATR, cm⁻¹) 3056, 2956, 2864, 2763, 1622, 1584, 1530, 1459, 1434, 1377, 1358, 1339, 1296, 1238, 1200, 1181, 1157, 1130, 1109, 1055, 1013, 933, 891, 816, 786, 768, 758, 700, 661, 631, 592, 524, 487, 438, 420. Melting Point: 260–261 °C. Elemental Analysis Anal. Found: C, 62.07; H, 8.00; N, 13.12. Calcd [C₄₄H₆₆FeN₈Zr]: C, 61.87; H, 7.79; N, 13.12.

Complex 3d [C₄₀H₆₂FeN₈Zr]. Proligand **1d** (46 mg, 0.09 mmol) was dissolved in tetrahydrofuran (0.2 mL), supplemented with solid Zr(NMe₂)₄ (23 mg, 0.09 mmol), and gently shaken until homogeneous. Upon standing overnight the product crystallized. The supernatant was removed, and the crystals were washed with tetrahydrofuran (3 × 0.1 mL) and dried under vacuum to obtain **3d**. Yield (77%, 53 mg). ¹H NMR (400 MHz, Toluene-*d*₈, -80 °C) δ 4.52 (br, 1H, Cp-*H*), 4.45 (br, 1H, Cp-*H*), 4.17 (br, 1H, Cp-*H*), 4.05 (br, 1H, Cp-*H*), 4.02 (br, 1H, Cp-*H*), 3.97 (br, 1H, Cp-*H*), 3.93 (br, 2H, Cp-*H*), 3.68 (br, 3H, guanidinate-N(CH₃)₂), 3.61 (br, 3H, guanidinate-N(CH₃)₂), 3.33 (br, 6H, guanidinate-N(CH₃)₂), 2.58 (br, 3H, Zr-N(CH₃)₂), 2.43 (br, 3H, Zr-N(CH₃)₂), 2.34 (br, 3H, Zr-N(CH₃)₂), 2.24–1.65 (m, 47H). ¹³C NMR (101 MHz, Toluene-*d*₈, 193 K) δ 171.8 (guanidinate-C), 169.6 (guanidinate-C), 107.4 (Cp-C-N), 106.4 (Cp-C-N), 67.9 (br, Cp-CH), 67.7 (Cp-CH), 66.0 (br, Cp-CH), 65.8 (br, Cp-CH), 64.6 (br, Cp-CH), 64.2 (Cp-CH), 63.8 (Cp-CH), 63.1 (Cp-CH), 59.0 (Cp-CH), 56.0 (N-C-Adamantyl), 53.7 (N-C-Adamantyl), 47.3 (Zr-N(CH₃)₂), 45.0 (-CH₂-), 44.6 (Zr-N(CH₃)₂), 41.6 (guanidinate-N(CH₃)₂), 39.7 (guanidinate-N(CH₃)₂), 39.2 (guanidinate-N(CH₃)₂), 36.9 (-CH₂-), 36.7 (-CH₂-), 30.5 (-CH-), 30.0 (-CH-). FT-IR (ATR, cm⁻¹) 2972, 2901, 2844, 2801, 2753, 1605, 1526, 1462, 1429, 1408, 1378, 1352, 1342, 1304, 1274, 1260, 1235, 1219, 1192, 1181, 1119, 1095, 1056, 1007, 979, 957, 922, 840, 815, 794, 759, 714, 695, 640, 617, 580, 515, 477, 422, 407. Melting Point: 237–238 °C. Elemental Analysis Anal. Found: C, 59.81; H, 7.64; N, 13.72. Calcd [C₄₀H₆₂FeN₈Zr]: C, 59.90; H, 7.79; N, 13.97.

Complex (4a) [C₂₈H₅₀FeN₈Hf]. Proligand **1a** (95 mg, 0.25 mmol) was dissolved in toluene (0.5 mL), and Hf(NMe₂)₄ (89 mg, 0.25 mmol) was added. The vial was shaken until homogeneous and allowed to stand for 4 h until crystalline material formed. The

supernatant was removed, and the residue was washed with additional toluene (0.15 mL) and dried under vacuum to obtain **4a**. Yield (115 mg, 63%). ¹H NMR (400 MHz, Toluene-*d*₈) δ 4.35 (br, 2H, Cp-*H*), 3.93 (br, 4H, Cp-*H*), 3.85 (br, 2H, Cp-*H*), 3.53 (br, 6H, Hf-N(CH₃)₂), 3.21 (br, 6H, Hf-N(CH₃)₂), 2.48 (s, 12H, guanidinate-N(CH₃)₂), 1.42 (s, 18H, -C(CH₃)₃). ¹³C NMR (101 MHz, Toluene-*d*₈) δ 170.7 (br, guanidinate-C), 106.0 (br, Cp-C-N), 65.6 (Cp-CH), 63.8 (Cp-CH), 53.8 (br, -C(CH₃)₃), 46.5 (Hf-N(CH₃)₂), 46.2 (Hf-N(CH₃)₂), 41.1 (br, guanidinate-N(CH₃)₂), 32.2 (-C(CH₃)₃). FT-IR (ATR, cm⁻¹) 3097, 3078, 2965, 2851, 2801, 2753, 1605, 1525, 1477, 1446, 1425, 1388, 1355, 1282, 1238, 1213, 1198, 1185, 1137, 1121, 1069, 1056, 1010, 959, 946, 923, 909, 836, 821, 799, 786, 764, 726, 685, 636, 617, 510, 487, 436. Melting Point: 222–223 °C. Elemental Analysis Anal. Found: C, 45.46; H, 6.59; N, 15.00. Calcd [C₂₈H₅₀FeN₈Hf]: C, 45.87; H, 6.87; N, 15.29.

Complex (4b) [C₃₈H₅₄FeN₈Hf]. Identical procedure for **3b** using Hf(NMe₂)₄ as the metal source. Yield of orange crystals (45 mg, 27%). ¹H NMR (400 MHz, Toluene-*d*₈) δ 6.73 (s, 4H), 4.31 (t, *J* = 2.0 Hz, 4H, Cp-*H*), 3.88 (t, *J* = 2.0 Hz, 4H, Cp-*H*), 2.89 (s, 12H, Hf-N(CH₃)₂), 2.35 (s, 12H, Aryl-CH₃), 2.17 (br, 12H, guanidinate-N(CH₃)₂), 2.15 (s, 6H, Aryl-CH₃). ¹³C NMR (101 MHz, Toluene-*d*₈) δ 168.1 (guanidinate-C), 143.9 (C_q), 132.9 (C_q), 131.9 (C_q), 129.1 (Aryl-CH), 108.6 (Cp-C-N), 64.2 (Cp-CH), 64.1 (Cp-CH), 44.2 (Hf-N(CH₃)₂), 38.3 (guanidinate-N(CH₃)₂), 20.8 (Aryl-CH₃), 19.1 (Aryl-CH₃). FT-IR (ATR, cm⁻¹) 3090, 2913, 2856, 2810, 2760, 1624, 1603, 1534, 1474, 1438, 1402, 1222, 1200, 1022, 1152, 1063, 1011, 946, 882, 851, 837, 813, 799, 764, 734, 683, 632, 615, 584, 554, 518, 499, 450, 433, 413. Melting Point: 268 °C. Elemental Analysis Anal. Found: C, 52.32; H, 6.41; N, 12.54. Calcd [C₃₈H₅₄FeN₈Hf]: C, 53.24; H, 6.35; N, 13.07.

Complex (4c) [C₄₄H₆₆FeN₈Hf]. Same procedure as that for **1c** using Hf(NMe₂)₄ as the metal source. The title compound crystallized as large orange crystalline chunks. Yield (111 mg, 69%). ¹H NMR (600 MHz, Toluene-*d*₈, 90 °C) δ 4.19 (t, *J* = 1.9 Hz, 4H, Cp-*H*), 3.89 (t, *J* = 1.8 Hz, 4H, Cp-*H*), 3.70 (hept, *J* = 6.9 Hz, 4H, Aryl-CH(CH₃)₂), 2.85 (s, 12H, Hf-N(CH₃)₂), 2.36 (s, 12H, guanidinate-N(CH₃)₂), 1.35 (d, *J* = 6.8 Hz, 12H, Aryl-CH(CH₃)₂), 1.33 (d, *J* = 6.8 Hz, 12H, Aryl-CH(CH₃)₂). ¹³C NMR (151 MHz, Toluene-*d*₈) δ 167.7 (guanidinate-C), 143.8 (C_q), 143.3 (C_q), 125.5 (Aryl-CH), 123.8 (Aryl-CH), 110.6 (Cp-C-N), 64.3 (Cp-CH), 62.7 (Cp-CH), 44.5 (Zr-N(CH₃)₂), 28.0 (guanidinate-N(CH₃)₂), 25.0 (Aryl-CH(CH₃)₂), 24.9 (Aryl-CH(CH₃)₂). FT-IR (ATR, cm⁻¹) 3058, 2956, 2866, 1620, 1584, 1529, 1458, 1434, 1376, 1326, 1273, 1252, 1234, 1199, 1142, 1107, 1057, 1021, 1000, 935, 792, 751, 701, 627, 484. Melting Point: 275–276 °C. Elemental Analysis Anal. Found: C, 56.31; H, 7.30; N, 11.90. Calcd [C₄₄H₆₆FeN₈Hf]: C, 56.14; H, 7.07; N, 11.90.

Complex 4d [C₄₀H₆₂FeN₈Hf]. Proligand **1d** (60 mg, 0.11 mmol) was dissolved in tetrahydrofuran (0.3 mL), solid Hf(NMe₂)₄ (40 mg, 0.11 mmol) was added, and the vial was shaken until homogeneous. Yellow crystals deposit overnight. The supernatant was removed, and the crystalline residue was washed with tetrahydrofuran (3 × 0.1 mL) and dried under vacuum to obtain **4d**. Yield (56%, 56 mg). ¹H NMR (400 MHz, Toluene-*d*₈, 233 K) δ 4.45 (s, 1H, Cp-*H*), 4.40 (s, 1H, Cp-*H*), 4.08 (s, 1H, Cp-*H*), 4.02 (s, 1H, Cp-*H*), 3.95 (s, 1H, Cp-*H*), 3.91 (s, 1H, Cp-*H*), 3.89 (s, 1H, Cp-*H*), 3.87 (s, 1H), 3.64 (m, 6H, Hf-N(CH₃)₂), 3.32 (s, 6H, Hf-N(CH₃)₂), 2.61 (s, 3H, guanidinate-N(CH₃)₂), 2.47 (s, 6H, guanidinate-N(CH₃)₂), 2.24–2.10 (m, 18H, guanidinate-N(CH₃)₂ + -CH₂- + -CH-), 1.96–1.93 (m, 3H, -CH₂-), 1.78–1.66 (m, 12H, -CH₂-). ¹³C NMR (101 MHz, Toluene-*d*₈, 233 K) δ 171.7 (guanidinate-C), 169.1 (guanidinate-C), 106.8 (Cp-C-N), 105.0 (Cp-C-N), 68.2 (Cp-CH), 65.9 (Cp-CH), 65.5 (Cp-CH), 64.6 (Cp-CH), 63.6 (Cp-CH), 63.1 (Cp-CH), 59.5 (Cp-CH), 55.7 (N-C-Adamantyl), 53.7 (N-C-Adamantyl), 47.2 (Hf-N(CH₃)₂), 46.8 (Hf-N(CH₃)₂), 46.3 (Hf-N(CH₃)₂), 45.1 (-CH₂-), 44.5 (guanidinate-N(CH₃)₂), 42.9 (-CH₂-), 41.7 (br, guanidinate-N(CH₃)₂), 40.0 (guanidinate-N(CH₃)₂), 39.4 (br, guanidinate-N(CH₃)₂), 37.1 (-CH₂-), 36.9 (-CH₂-), 30.7 (-CH-), 30.2 (-CH-). FT-IR (ATR, cm⁻¹) 2902, 2848, 2804, 2757, 2742, 1601, 1533, 1516, 1477, 1462, 1446, 1425, 1407, 1390,

1354, 1344, 1302, 1279, 1218, 1191, 1133, 1117, 1096, 1053, 1020, 1009, 955, 946, 918, 837, 820, 794, 758, 772, 720, 707, 696, 642, 620, 577, 513, 502, 490, 473, 427, 416. Melting Point: 243–244 °C. Elemental Analysis Anal. Found: C, 53.92; H, 6.95; N, 12.66. Calcd [C₄₀H₆₂FeN₈Hf]: C, 54.02; H, 7.03; N, 12.60.

[C₁₉H₃₂FeN₆Zr] (5) **2b**. (52 mg, 0.1 mmol) and Zr(NMe₂)₄ (56 mg, 0.21 mmol) were dissolved in C₆D₆ (0.8 mL) and heated to 75 °C for 68 h. ¹H NMR (400 MHz, Benzene-*d*₆) δ 4.17 (t, *J* = 1.9 Hz, 2H, Cp-*H*), 4.13 (t, *J* = 1.9 Hz, 2H, Cp-*H*), 3.87 (t, *J* = 1.9 Hz, 2H, Cp-*H*), 3.77 (t, *J* = 1.9 Hz, 2H, Cp-*H*), 2.91 (s, 18H, Zr-N(CH₃)₂), 2.55 (s, 6H, guanidinate-N(CH₃)₂). ¹³C NMR (101 MHz, Benzene-*d*₆) δ 169.1 (guanidinate-C), 107.0 (Cp-C-N), 99.2 (Cp-C-N), 68.6 (Cp-CH), 68.3 (Cp-CH), 67.5 (Cp-CH), 65.0 (Cp-CH), 45.3 (guanidinate-N(CH₃)₂), 42.1 (Zr-N(CH₃)₂). The free guanidine [C₁₃H₁₅FeN₃] (6) can be isolated by hydrolysis of the reaction mixture. **2b** (94 mg, 0.19 mmol) and a slight excess of Zr(NMe₂)₄ (135 mg, 0.5 mmol) in C₆D₆ (1.2 mL) were heated in a valved NMR tube for 24 h at 75 °C. The solution was cooled and poured into wet ice-cold dichloromethane (15 mL) under vigorous stirring. After 15 min a spatula tip of MgSO₄ was added, the resulting suspension was filtered through a plug of diatomaceous earth to eliminate MgSO₄/ZrO₂ and evaporated under reduced pressure. The orange colored residue was crushed in pentane (5 mL), filtered and washed with additional pentane (3 × 1 mL) to afford the title compound. Yield of orange microcrystalline solid (15 mg, 56%). ¹H NMR (500 MHz, Benzene-*d*₆) δ 4.16 (s, 1H, N-*H*), 4.08 (br, 4H, Cp-*H*), 3.83 (m, 4H, Cp-*H*), 2.59 (s, 6H, guanidine-N(CH₃)₂). ¹³C NMR (126 MHz, Benzene-*d*₆) δ 158.4 (guanidine-C), 108.2 (Cp-C-N), 89.4 (Cp-C-N), 69.6 (Cp-CH), 69.4 (Cp-CH), 68.5 (Cp-CH), 65.3 (Cp-CH), 38.5 (guanidinate-N(CH₃)₂). FT-IR (ATR, cm⁻¹) 3068, 2917, 1569, 1499, 1452, 1433, 1357, 1282, 1206, 1184, 1136, 1053, 1035, 1025, 914, 897, 872, 844, 816, 799, 791, 733, 710, 652, 598, 524, 473, 450, 409. Melting Point: 195–196 °C (dec.). HR-MS (ESI) *m/z* 270.0695 [Calculated for C₁₃H₁₆FeN₃⁺ 270.0688]f

[C₂₇H₄₇N₆Zr] (7) Zr(NMe₂)₃[MesitylNC(NMe₂)NMe₂]. The title compound can be independently synthesized from *N,N'*-dimesityl carbodiimide³¹ (0.42 mmol, 118 mg) and Zr(NMe₂)₄ (0.42 mmol, 114 mg) in C₆D₆ but was not isolated. ¹H NMR (400 MHz, Benzene-*d*₆) δ 6.85 (s, 4H, Aryl-*H*), 2.96 (s, 18H, Zr-N(CH₃)₂), 2.31 (s, 12H, Aryl-CH₃), 2.22 (s, 6H, Aryl-CH₃), 1.94 (s, 6H, guanidinate-N(CH₃)₂). ¹³C NMR (101 MHz, Benzene-*d*₆) δ 167.4 (guanidinate-C), 143.9 (C_q), 132.7 (C_q), 131.8 (C_q), 129.4 (Aryl-CH), 42.5 (Zr-N(CH₃)₂), 37.5 (guanidinate-N(CH₃)₂), 20.9 (Aryl-CH₃), 19.2 (Aryl-CH₃). Complex 7 in benzene solution was poured into wet ice-cooled dichloromethane (5 mL) and allowed to stir for 15 min. The solution was syringe filtered (0.2 μm), the solvent was evaporated under reduced pressure, and the resulting white residue was recrystallized from pentane to obtain free *N,N*-dimethyl-*N',N''*-dimesityl-guanidine [C₂₁H₂₉N₃] (8) as colorless plates. Yield (10 mg, 7%). ¹H NMR (500 MHz, Benzene-*d*₆) δ 6.96 (br, 2H, Aryl-*H*), 6.63 (br, 2H, Aryl-*H*), 4.83 (br, 1H, N-*H*), 2.50 (s, 6H, -N(CH₃)₂), 2.39 (br, 6H, Aryl-CH₃), 2.27 (br, 3H, Aryl-CH₃), 2.10 (br, 3H, Aryl-CH₃), 2.03 (br, 5H, Aryl-CH₃). ¹³C NMR (126 MHz, Benzene-*d*₆) δ 151.7 (guanidine-C), 135.9 (br, C_q), 134.7 (br, C_q), 134.4 (br, C_q), 130.8 (br, C_q), 129.5 (Aryl-CH), 39.2 (-N(CH₃)₂), 20.9 (Aryl-CH₃), 18.9 (Aryl-CH₃), 18.6 (Aryl-CH₃). FT-IR (ATR, cm⁻¹) 3345, 2917, 2854, 1619, 1600, 1473, 1446, 1367, 1265, 1200, 1143, 1054, 1034, 996, 857, 810, 722, 694. Melting Point: 103–104 °C. HR-MS (ESI) *m/z* 324.2432 [Calculated for C₂₁H₃₀N₃⁺ 324.2434].

[C₄₆H₇₈FeN₁₂Zr₂] (9). Only ¹H and ¹³C NMR data are reported for this compound. ¹H NMR (500 MHz, Benzene-*d*₆) δ 6.82 (s, 4H, Aryl-*H*), 4.37 (t, *J* = 1.9 Hz, 4H, Cp-*H*), 4.17 (t, *J* = 1.9 Hz, 4H, Cp-*H*), 3.17 (s, 36H, Zr-N(CH₃)₂), 2.23 (s, 12H, Aryl-CH₃), 2.20 (s, 6H, Aryl-CH₃), 2.09 (s, 12H, guanidinate-N(CH₃)₂). ¹³C NMR (126 MHz, Benzene-*d*₆) δ 170.0 (guanidinate-C), 132.2 (C_q), 129.2 (Aryl-CH), 144.0 (C_q), 128.5 (C_q), 107.2 (Cp-C-N), 67.2 (Cp-CH), 64.8 (Cp-CH), 43.2 (Zr-N(CH₃)₂), 38.7 (guanidinate-N(CH₃)₂), 20.9 (Aryl-CH₃), 19.1 (Aryl-CH₃).

[C₁₇H₄₂N₆Zr] (10) Zr(NMe₂)₃[*tert*-butylNC(NMe₂)N-*tert*-butyl]. The title compound can be independently synthesized from commercially available *N,N'*-di-*tert*-butylcarbodiimide (25 mg, 0.16 mmol) and Zr(NMe₂)₄ (44 mg, 0.16 mmol) in C₆D₆ solution (0.8 mL) but was not isolated. ¹H NMR (400 MHz, Benzene-*d*₆) δ 3.11 (s, 18H, Zr-N(CH₃)₂), 2.36 (s, 6H, guanidinate-N(CH₃)₂), 1.21 (s, 18H, -C(CH₃)₃). ¹³C NMR (101 MHz, Benzene-*d*₆) δ 170.5 (guanidinate-C), 54.0 (-C(CH₃)₃), 43.3 (Zr-N(CH₃)₂), 41.2 (guanidinate-N(CH₃)₂), 32.0 (-C(CH₃)₃). After the NMR analysis, the benzene solution was poured into wet ice-cold dichloromethane (15 mL). After the solution stirred for 15 min, a spatula tip of MgSO₄ was added and the suspension was filtered through a plug of diatomaceous earth to remove MgSO₄/ZrO₂. The solvent was evaporated under reduced pressure, and the residue recrystallized from benzene to obtain guanidine [C₁₁H₂₅N₃] (11). Yield of white solid (7 mg, 22%). ¹H NMR (500 MHz, Chloroform-*d*) δ 2.90 (s, 6H, -N(CH₃)₂), 1.90 (s, br, 1H, N-*H*), 1.42 (s, 18H, -C(CH₃)₃). ¹³C NMR (126 MHz, Chloroform-*d*) δ 160.7 (guanidine-C), 55.6 (-C(CH₃)₃), 41.7 (-N(CH₃)₂), 30.0 (-C(CH₃)₃). FT-IR (ATR, cm⁻¹) 2962, 2870, 1625, 1595, 1529, 1490, 1464, 1394, 1366, 1282, 1151, 1196, 1096, 1081, 1057, 1041, 959, 817, 681, 630, 614, 598, 547, 451. Melting Point: 119–121 °C. HR-MS (ESI) *m/z* 200.2128 [Calculated for C₁₁H₂₆N₃⁺ 200.2127].

■ ASSOCIATED CONTENT

📄 Supporting Information

The Supporting Information is available free of charge on the ACS Publications website at DOI: 10.1021/acs.organomet.9b00336.

Details of experimental procedures, UV-vis spectra, NMR spectra, cyclic voltammetry, kinetic plots, steric plots (PDF)

Accession Codes

CCDC 1909323–1909339 contain the supplementary crystallographic data for this paper. These data can be obtained free of charge via www.ccdc.cam.ac.uk/data_request/cif, or by emailing data_request@ccdc.cam.ac.uk, or by contacting The Cambridge Crystallographic Data Centre, 12 Union Road, Cambridge CB2 1EZ, UK; fax: +44 1223 336033.

■ AUTHOR INFORMATION

Corresponding Author

*E-mail: rajones@cm.utexas.edu.

ORCID

Richard A. Jones: 0000-0003-4174-6530

Funding

The project that gave rise to these results received the support of “la Caixa” Banking Foundation (LCF/BQ/AA17/11610005) in the form of a fellowship for O.E.P. We thank the Welch Foundation (F-816) for support. The Bruker Avance III HD 500 was purchased with funds from an NIH grant (1 S10 OD021508-01).

Notes

The authors declare no competing financial interest.

■ ACKNOWLEDGMENTS

We thank Professor M. J. Rose and C. Joseph for permission to use their electrochemical instrumentation and technical guidance. We also thank J. Chen at the Texas Center for Electrochemistry for useful advice.

REFERENCES

- (1) Shafir, A.; Power, M. P.; Whitener, G. D.; Arnold, J. *Organometallics* **2000**, *19* (19), 3978–3982.
- (2) Shafir, A.; Power, M. P.; Whitener, G. D.; Arnold, J. *Organometallics* **2001**, *20* (7), 1365–1369.
- (3) Brosmer, J. L.; Huang, W.; Diaconescu, P. L. *Organometallics* **2017**, *36* (23), 4643–4648.
- (4) Pick, F. S.; Thompson, J. R.; Savard, D. S.; Leznoff, D. B.; Fryzuk, M. D. *Inorg. Chem.* **2016**, *55* (8), 4059–4067.
- (5) Halcovitch, N. R.; Fryzuk, M. D. *Aust. J. Chem.* **2016**, *69* (5), 555–560.
- (6) Shafir, A.; Arnold, J. *Inorg. Chim. Acta* **2003**, *345*, 216–220.
- (7) Shafir, A.; Fiedler, D.; Arnold, J. *J. Chem. Soc. Dalton Trans.* **2002**, No. 4, 555–560.
- (8) Quan, S. M.; Wei, J.; Diaconescu, P. L. *Organometallics* **2017**, *36* (22), 4451–4457.
- (9) Gibson, V. C.; Long, N. J.; Marshall, E. L.; Oxford, P. J.; White, A. J. P.; Williams, D. J. *J. Chem. Soc., Dalton Trans.* **2001**, *1* (i), 1162–1164.
- (10) Abubekurov, M.; Khan, S. I.; Diaconescu, P. L. *Organometallics* **2017**, *36* (22), 4394–4402.
- (11) Klapp, L. R. R.; Bruhn, C.; Leibold, M.; Siemeling, U. *Organometallics* **2013**, *32* (20), 5862–5872.
- (12) Heinze, K.; Lang, H. *Organometallics* **2013**, *32* (20), 5623–5625.
- (13) Wilkinson, G.; Rosenblum, M.; Whiting, M. C.; Woodward, R. B. *J. Am. Chem. Soc.* **1952**, *74* (8), 2125–2126.
- (14) Dunitz, J. D.; Orgel, L. E.; Rich, A. *Acta Crystallogr.* **1956**, *9* (4), 373–375.
- (15) Togni, A.; Hayashi, T. *Ferrocenes*; VCH: 1995.
- (16) Astruc, D. *Eur. J. Inorg. Chem.* **2017**, *2017* (1), 6–29.
- (17) Huang, W.; Diaconescu, P. L. *Inorg. Chem.* **2016**, *55* (20), 10013–10023.
- (18) Arumugam, K.; Varnado, C. D.; Sproules, S.; Lynch, V. M.; Bielawski, C. W. *Chem. - Eur. J.* **2013**, *19* (33), 10866–10875.
- (19) Gregson, C. K. A.; Gibson, V. C.; Long, N. J.; Marshall, E. L.; Oxford, P. J.; White, A. J. P. *J. Am. Chem. Soc.* **2006**, *128* (23), 7410–7411.
- (20) Dai, R.; Diaconescu, P. L. *Dalt. Trans.* **2019**, *48*, 2996–3002.
- (21) Schlögl, K.; Mechtler, H. *Angew. Chem.* **1966**, *78* (11), 606.
- (22) Sola, A.; Orenes, R. A.; Tàrraga, A.; Molina, P. *Tetrahedron Lett.* **2016**, *57* (9), 1048–1052.
- (23) Otón, F.; Espinosa, A.; Tàrraga, A.; De Arellano, C. R.; Molina, P. *Chem. - Eur. J.* **2007**, *13* (20), 5742–5752.
- (24) Oton, F.; Espinosa, A.; Tarraga, A.; Molina, P. *Organometallics* **2007**, *26* (25), 6234–6242.
- (25) Gurskaya, L.; Bagryanskaya, I.; Amosov, E.; Kazantsev, M.; Politanskaya, L.; Zaytseva, E.; Bagryanskaya, E.; Chernonosov, A.; Tretyakov, E. *Tetrahedron* **2018**, *74* (15), 1942–1950.
- (26) Bagryanskaya, I.; Fedin, M.; Gorbunov, D.; Gritsan, N.; Gurskaya, L.; Kazantsev, M.; Polienko, Y.; Stass, D.; Tretyakov, E. *Tetrahedron Lett.* **2017**, *58* (5), 478–481.
- (27) Álvarez-Rodríguez, L.; Cabeza, J. A.; García-Álvarez, P.; Polo, D. *Coord. Chem. Rev.* **2015**, *300*, 1–28.
- (28) Hill, N. J.; Findlater, M.; Cowley, A. H. *Dalt. Trans.* **2005**, No. 19, 3229–3234.
- (29) Edelmann, F. T. *Chapter 3 Advances in the Coordination Chemistry of Amidinate and Guanidinate Ligands*; Elsevier Inc.: 2008; Vol. 57.
- (30) Chlupatý, T.; Růžička, A. *Coord. Chem. Rev.* **2016**, *314*, 103–113.
- (31) Peddaraio, T.; Baishya, A.; Barman, M. K.; Kumar, A.; Nembenna, S. *New J. Chem.* **2016**, *40* (9), 7627–7636.
- (32) Maity, A. K.; Fortier, S.; Griego, L.; Metta-Magaña, A. J. *Inorg. Chem.* **2014**, *53* (15), 8155–8164.
- (33) Findlater, M.; Hill, N. J.; Cowley, A. H. *Dalt. Trans.* **2008**, No. 33, 4419–4423.
- (34) Gordon, P. G.; Yap, G. P. A.; Barry, S. T. *J. Chem. Crystallogr.* **2011**, *41* (3), 375–378.
- (35) Goj, O.; Haufe, G.; Fröhlich, R. *Acta Crystallogr., Sect. C: Cryst. Struct. Commun.* **1996**, *52* (6), 1554–1556.
- (36) Ulrich, H. *Chemistry and Technology of Carbodiimides*; John Wiley & Sons Ltd.: 2007.
- (37) Kaspi-Kaneti, A. W.; Tuvi-Arad, I. *Organometallics* **2018**, *37* (19), 3314–3321.
- (38) Sharma, B.; Callaway, T. M.; Lamb, A. C.; Steren, C. A.; Chen, S. J.; Xue, Z. L. *Inorg. Chem.* **2013**, *52* (19), 11409–11421.
- (39) Cook, T. M.; Steren, C. A.; Xue, Z. L. *Dalt. Trans.* **2018**, *47* (32), 11030–11040.
- (40) Dai, R.; Lai, A.; Alexandrova, A. N.; Diaconescu, P. L. *Organometallics* **2018**, *37* (21), 4040–4047.
- (41) Falivene, L.; Credendino, R.; Poater, A.; Petta, A.; Serra, L.; Oliva, R.; Scarano, V.; Cavallo, L. *Organometallics* **2016**, *35* (13), 2286–2293.
- (42) For the sake of completion, metalation with $\text{Ti}(\text{NMe}_2)_4$ has been attempted. In our hands we have only recovered impure and poorly defined products. From hexanes we were able to recover a thin crystalline plate of a bimetallic cluster of formula $[\text{C}_{49}\text{H}_{79}\text{Fe}_2\text{N}_{13}\text{O}_2\text{Ti}_2]$; see SI 36 for ORTEP diagram.
- (43) Zeitler, H. E.; Kaminsky, W. A.; Goldberg, K. I. *Organometallics* **2018**, *37* (21), 3644–3648.
- (44) Lloveras, V.; Caballero, A.; Tàrraga, A.; Velasco, M. D.; Espinosa, A.; Wurst, K.; Evans, D. J.; Vidal-Gancedo, J.; Rovira, C.; Molina, P.; Veciana, J. *Eur. J. Inorg. Chem.* **2005**, *2005* (12), 2436–2450.
- (45) Sola, A.; Orenes, R. A.; García, M. Á.; Claramunt, R. M.; Alkorta, I.; Elguero, J.; Tàrraga, A.; Molina, P. *Inorg. Chem.* **2011**, *50* (9), 4212–4220.
- (46) Barbey, G.; Caullet, C. *Tetrahedron Lett.* **1977**, *18* (45), 3937–3938.
- (47) Knolker, H. J.; Braxmeier, T.; Schlechtingen, G. *Angew. Chem., Int. Ed. Engl.* **1995**, *34* (22), 2497–2500.